

Supporting Information

In-situ synthesis of polyaniline/carbon nanotube composites in carbonised wood scaffold for high performance supercapacitors

Wei Wu, Xin Wang, Yuanyuan Deng, Cui Zhou, Ziheng Wang, Minglong Zhang,

Xianjun Li, Yiqiang Wu, Yongfeng Luo, Daoyong Chen

A: Calculate the single-electrode capacitance under the three-electrode system

The volume and specific capacitance of a single electrode in a three-electrode cell configuration can be calculated according to their GCD curves by the following equations:

$$C_{(Volume)} = \frac{I \times \Delta t}{V \times \Delta U} \quad (1)$$

$$C_{(Specific)} = \frac{I \times \Delta t}{m \times \Delta U} \quad (2)$$

where I is the discharge current, Δt is the discharge time, ΔU is the potential window of the discharge process, V is the effective volume of the electrode, and m is the mass of active material.

B: Calculate the asymmetric supercapacitor capacitance under the two-electrode system

The volume and specific capacitance of asymmetric supercapacitor under the two-electrode system can be calculated according to their GCD curves by the following equations:

$$C_{(Volume)} = \frac{I \times \Delta t}{V \times \Delta U} \quad (3)$$

$$C_{(Specific)} = \frac{I \times \Delta t}{m \times \Delta U} \quad (4)$$

In this case, V is the total volume of the two electrodes, and m is the total mass of the device.

The energy density (E) and power density (P) were calculated according to the following equations respectively:

$$E = \frac{1}{2} \times C \times \Delta U^2 \quad (6)$$

$$P = \frac{E}{\Delta t} \quad (7)$$

where C is the volume or specific capacitance of the asymmetric supercapacitor, Δt and ΔU are the discharge time and potential window of the discharge process.

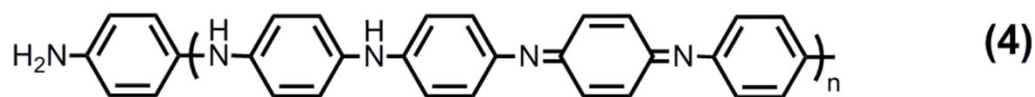
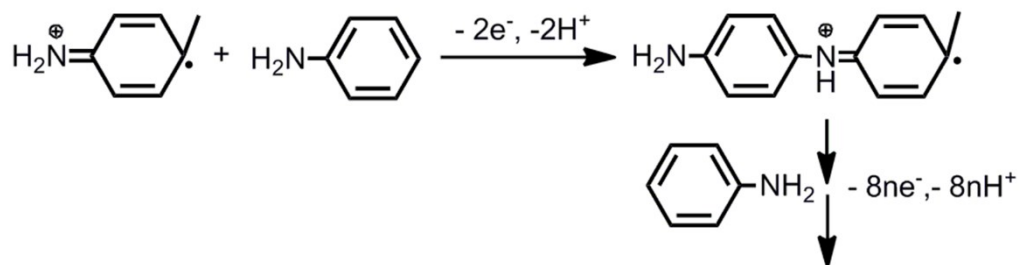
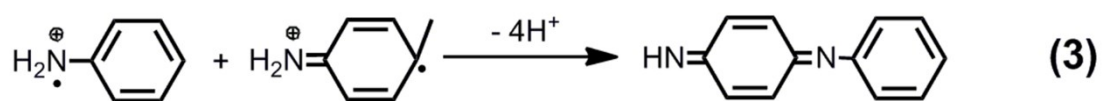


Fig. S1: The synthesis mechanism of electrodeposited PANI.

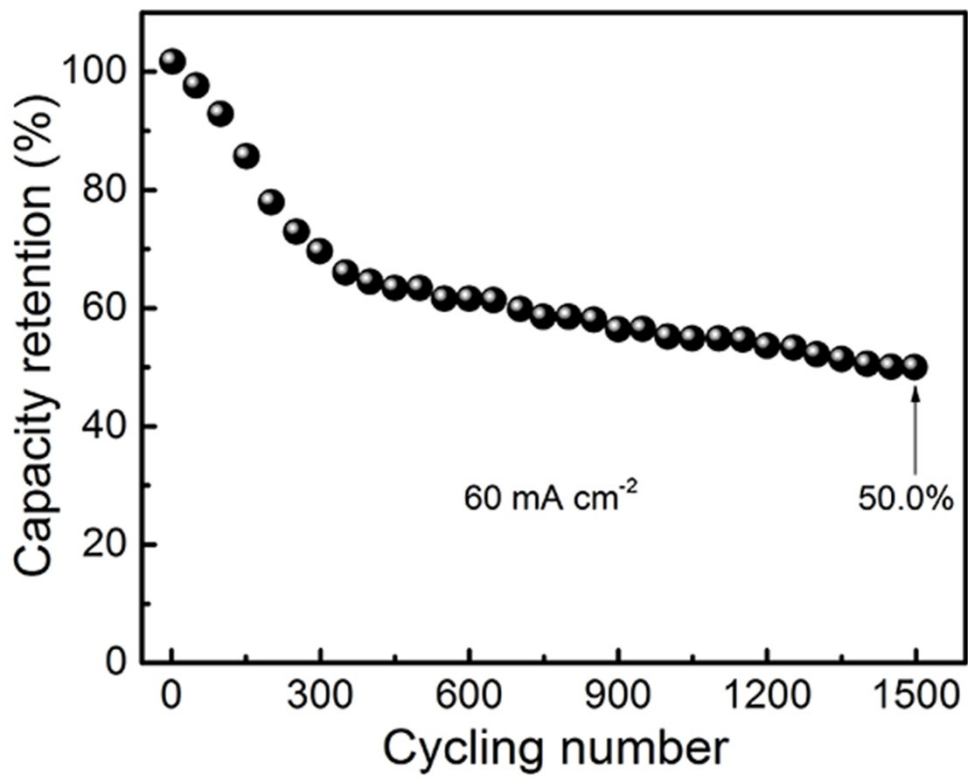


Fig. S2: The cyclability of the PANI@AWC slice.

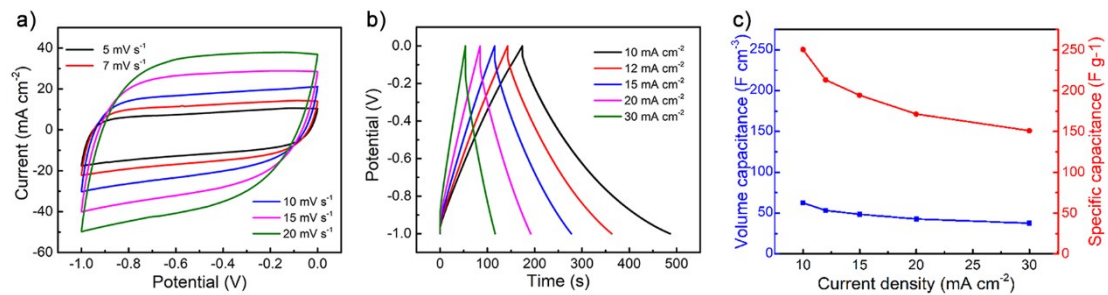


Fig. S3: Electrochemical characteristics of CNT/AWC slices: (a) CV curves at various scan rates, (b) GCD curves at different current densities, (c) the volume and mass specific capacitance at different current densities.

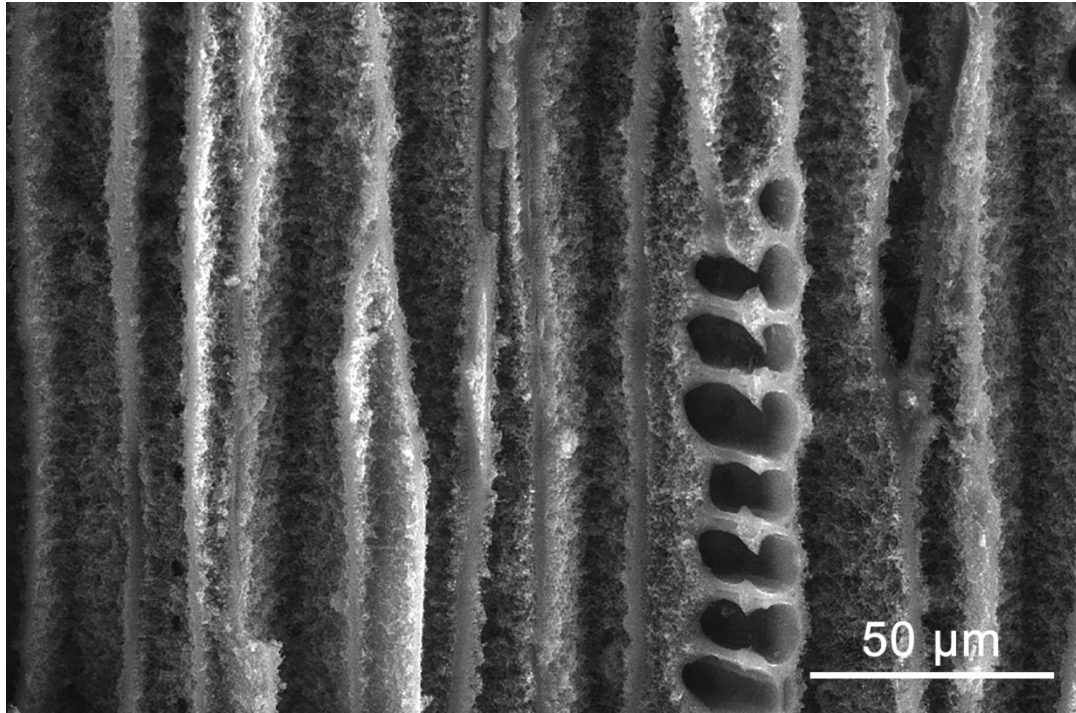


Fig. S4: SEM image of the cross-sectional-view of an PANI@CNT/AWC slices

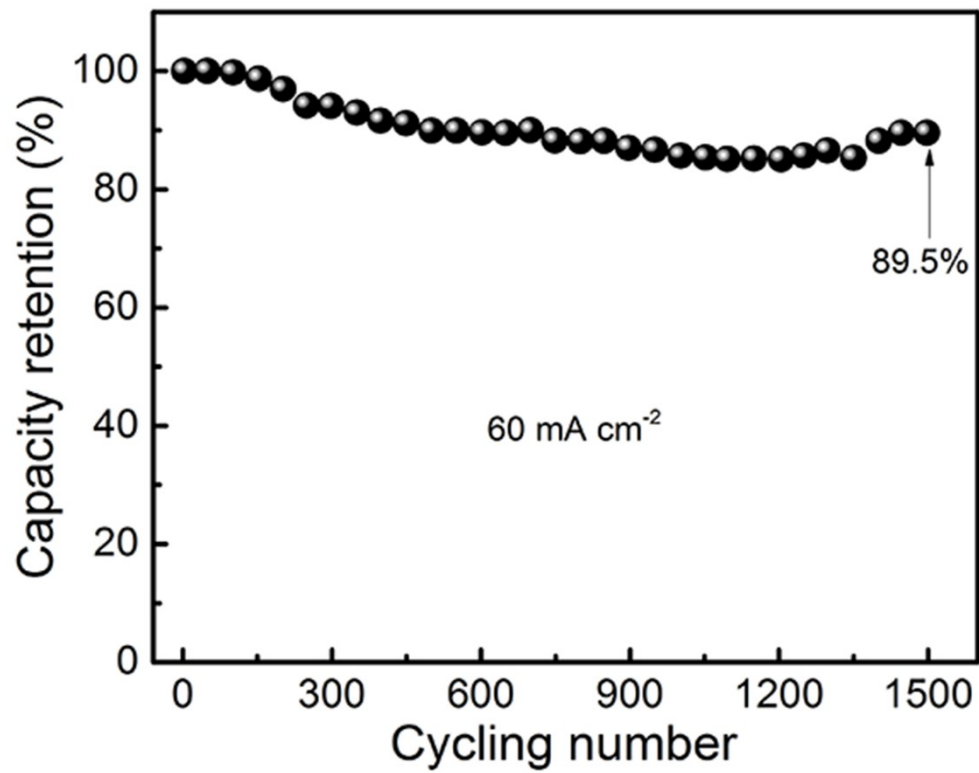


Fig. S5: The cyclability of the PANI@CNT/AWC slice.

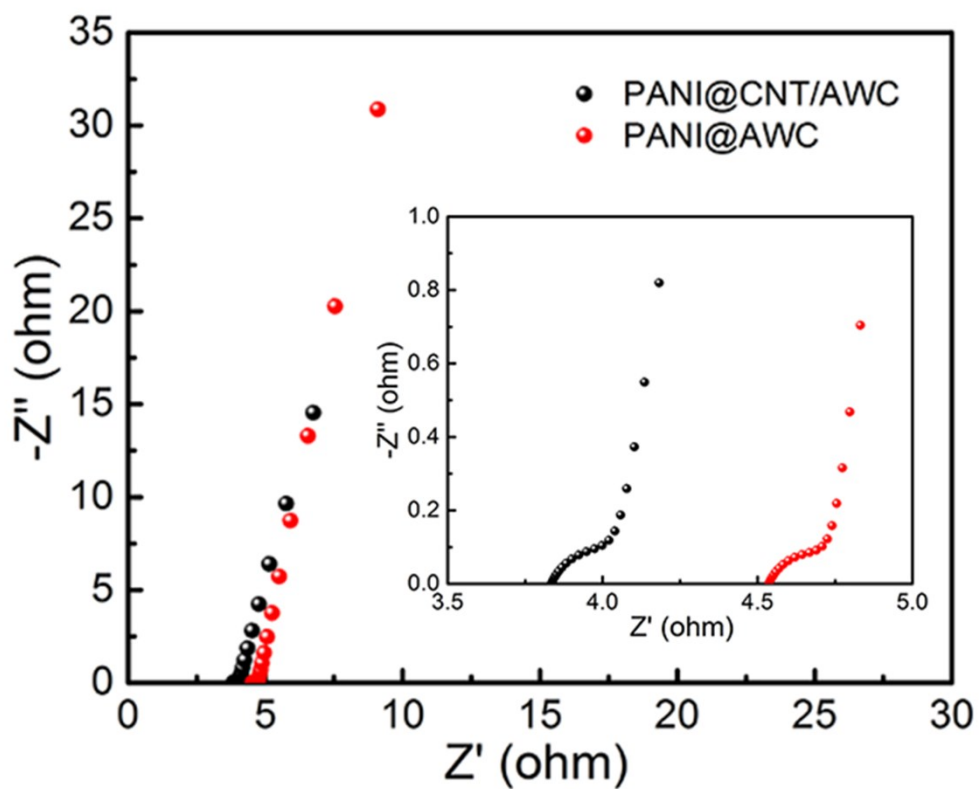


Fig. S6: Nyquist plots of the PANI@CNT/AWC and PANI@AWC slices; the inset graph is the magnified image.

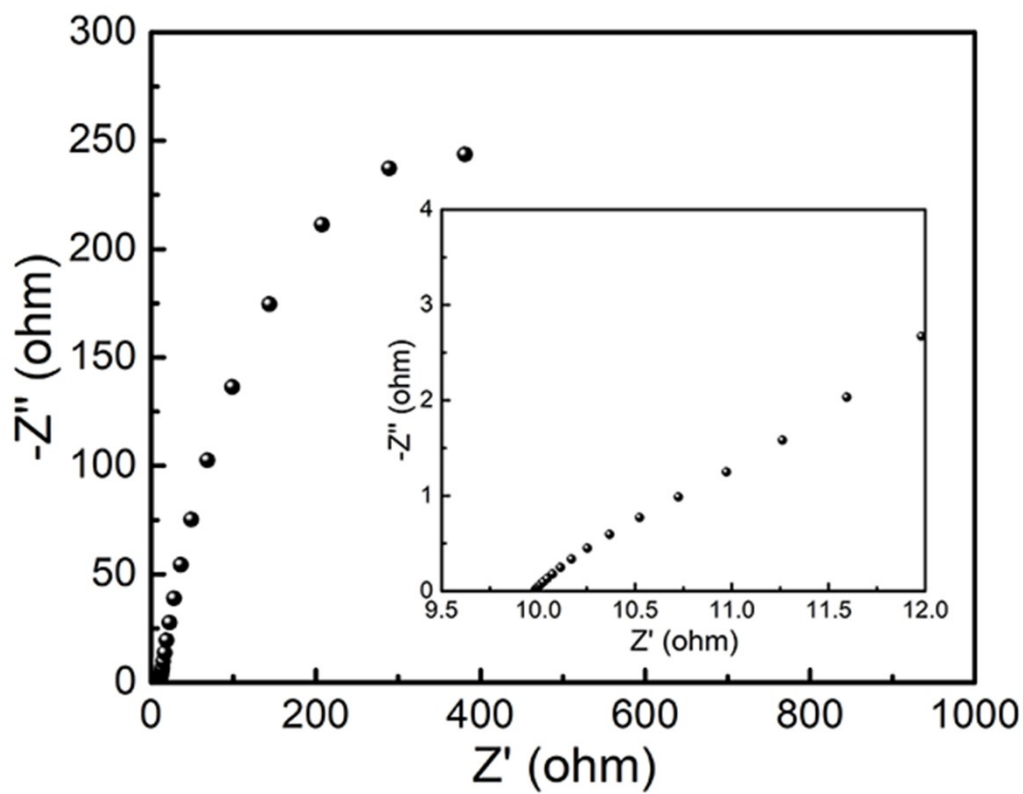


Fig. S7: Nyquist plots of the ASC device; the inset graph is the magnified image

Table S1: The comparison of specific energy density and cycling stability between PANI@CNT/AWC//CNT /AWC ASC device and other supercapacitors.

Material name	Specific capacitance	Energy density	Cycling stability	Reference
AWC// MnO ₂ @WC ASC	14.4 F cm ⁻³ at 1 mA cm ⁻²	16 Wh kg ⁻¹	93% (10000)	Ref. 1
CW/PVA-KOH/Co(OH) ₂ @CW	34.8 F g ⁻¹ at 1 mA cm ⁻²	10.87 Wh kg ⁻¹	85% (10000)	Ref. 2
CA//CA-PANI	64.5 F g ⁻¹ at 2.8 A g ⁻¹	24.4 Wh kg ⁻¹	98% (3000)	Ref. 3
CNFs/CNTs/PANI SC	57 F g ⁻¹ at 0.5 A g ⁻¹	5.1 Wh kg ⁻¹	92% (10000)	Ref. 4
PANI/NCNT SC	128 F g ⁻¹ at 2.47 A g ⁻¹	11.11 Wh kg ⁻¹	92% (10000)	Ref. 5
PANI-CNT SC	80 F g ⁻¹ at 0.5 A g ⁻¹	7.11 Wh kg ⁻¹	81% (1000)	Ref. 6
PANI/RGO wood SC	0.89 F cm ⁻² at 1 mV s ⁻¹	107.70 mWh cm ⁻²	88.11% (5000)	Ref. 7
WTSS/Ppy SC	0.61 F cm ⁻² at 1 mV s ⁻¹	48.83 mWh cm ⁻²	87.5% (5000)	Ref. 8
PANI/P-MWCNT SC	95.7 F g ⁻¹ at 0.5 A g ⁻¹	8.2 Wh kg ⁻¹	71.8% (2000)	Ref. 9
CDP-Pani/CNT SC	107.4 F g ⁻¹ at 1 A g ⁻¹	21.0 Wh kg ⁻¹	97% (5000)	Ref. 10
RGO/UCNTs/PANI	53.1 F g ⁻¹ at 0.5 A g ⁻¹	7.4 Wh kg ⁻¹	80.5% (2000)	Ref. 11
PANI-CNT/ExGP	79.9 F g ⁻¹ at 1 A g ⁻¹	7.1 Wh kg ⁻¹	77.6% (3000)	Ref. 12
PANI@CNT/AWC ASC	90.9 F g ⁻¹ at 5 mA cm ⁻²	40.5 Wh kg ⁻¹	93.74% (10000)	This work

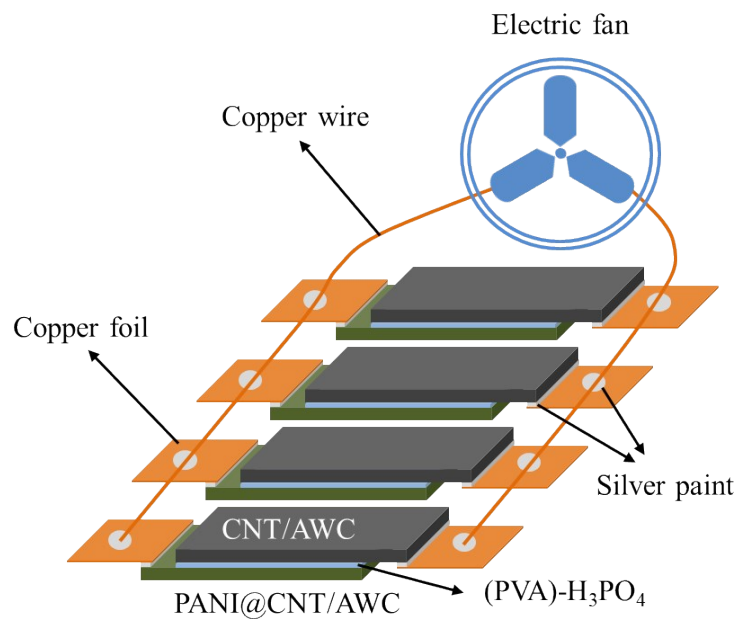


Figure S8: Schematic diagram of connections between four parallel supercapacitors and external circuits

REFERENCES

1. C. Chen, Y. Zhang, Y. Li, J. Dai, J. Song, Y. Yao, Y. Gong, I. Kierzewski, J. Xie and L. Hu, *Energy & Environmental Science*, 2017, 10, 538-545.
2. Y. Wang, X. Lin, T. Liu, H. Chen, S. Chen, Z. Jiang, J. Liu, J. Huang and M. Liu, *Advanced Functional Materials*, 2018, 28.
3. V. Sahu, R. B. Marichi, G. Singh and R. K. Sharma, *Electrochimica Acta*, 2017, 240, 146-154.
4. F. Miao, C. Shao, X. Li, K. Wang, N. Lu and Y. Liu, *ACS Sustainable Chemistry Engineering*, 2016, 4, 1689-1696.
5. R. Malik, L. Zhang, C. McConnell, M. Schott, Y.-Y. Hsieh, R. Noga, N. T. Alvarez and V. Shanov, *Carbon*, 2017, 116, 579-590.
6. S. K. Simotwo, C. DelRe and V. Kalra, *ACS Applied Materials Interfaces*, 2016, 8, 21261-21269.
7. S. Lyu, Y. Chen, S. Han, L. Guo, N. Yang and S. Wang, *RSC Advances*, 2017, 7, 54806-54812.
8. S. Lv, F. Fu, S. Wang, J. Huang and L. Hu, *Rsc Adv*, 2015, 5, 2813-2818.
9. Q. Liu, Z. Bai, J. Fan, Z. Sun, H. Mi, Q. Zhang and J. Qiu, *Applied Surface Science*, 2018, 436, 189-197.
10. W. Zhang, Y. Kong, X. Jin, B. Yan, G. Diao and Y. Piao, *Electrochimica Acta*, 2020, 331, 135345.
11. Y. Huang, J. Zhou, N. Gao, Z. Yin, H. Zhou, X. Yang and Y. Kuang, *Electrochimica Acta*, 2018, 269, 649-656.

12. H. Zhou, X. Zhi and H.-J. Zhai, *International Journal of Hydrogen Energy*, 2018, 43, 18339-18348.